Non-intrusive reduced order models for partitioned fluid-structure interactions

Azzeddine Tiba, Thibault Dairay, Florian de Vuyst, Iraj Mortazavi, Juan-Pedro Berro Ramirez

ERCOFTAC Symposium on "Multiphysics critical flow dynamics involving moving/ deformable structures with design applications", Toulouse, France, 7-8-9 June 2023

Non-intrusive reduced order models for partitioned fluid-structure interactions

Azzeddine TIBA[1], Thibault DAIRAY[2], Florian DE VUYST[3], Iraj MORTAZAVI[1], Juan Pedro BERRO RAMIREZ[4]

[1] *M2N, CNAM Paris, Rue Conté, 75003, Paris*
[2] *Manufacture Française des Pneumatiques Michelin, Place des Carmes-Dechaux, 63000, Clermont-Ferrand*
[3] *Université de Technologie de Compiègne, CNRS, laboratoire BMBI UMR 7338, Rue du docteur Schweitzer, 60203 Compiègne*
[4] *Altair Engineering France, Rue de la Renaissance, 92160 Antony*

Abstract.

The main goal of this research is to develop a data-driven reduced order model (ROM) strategy from high-fidelity simulation result data of a full order model (FOM). The goal is to predict at lower computational cost the time evolution of solutions of Fluid-Structure Interaction (FSI) problems. For some FSI applications like tire/water interaction, the FOM solid model (often chosen as quasi-static) can take far more computational time than the HF fluid one. In this context, for the sake of performance one could only derive a reduced-order model for the structure and try to achieve a partitioned HF fluid solver coupled with a ROM solid one. In this paper, we present a data-driven partitioned ROM on a study case involving a simplified 1D-1D FSI problem representing an axisymmetric elastic model of an arterial vessel, coupled with an incompressible fluid flow. We derive a purely data-driven solid ROM for FOM fluid - ROM structure partitioned coupling and present early results.

Key words: Reduced order model, fluid-structure interaction, partitioned coupling, FOM-ROM coupling, data-driven model.

1 Introduction

Fluid-structure interaction (FSI) is the class of mechanical problems dealing with the coupling and interactions between a deformable solid body subject to a fluid loading and a fluid flow. FSI simulations with strong two-way coupling are usually computationally expensive, due to both kinematics and dynamics coupling of the two systems, and the structure of the spatiotemporal dynamics. Although Full Order Models (FOM) are available and can be discretized using popular numerical methods (*e.g.* finite elements, finite volumes, particle methods ...), the computational cost associated with the simulations is often very high and makes them intractable to predict High-Fidelity (HF) solutions on long-term time periods. In this paper, we

will especially focus on simulations based on moving fluid domain methods, the most popular one being the Arbitrary Lagrangian-Eulerian (ALE) method [8].
When solving FSI problems, two main strategies arise, namely the partitioned and monolithic approaches. In the monolithic approach, both the solid and fluid systems are considered as a whole, and the governing equations for both the physics are solved at once, each time step. While this approach is more robust to the nature of the coupling, due to its abilities to satisfy the coupling conditions exactly [18, 1, 14, 10], they represent significant computational and mathematical difficulties, due to the complexity of solving both fluid *and* solid equations simultaneously, while not allowing for the use of well-validated existing structural and fluid solvers.
Partitioned approaches however tackle these challenges with strategies that involve solving the different physics separately, allowing for the use and coupling of available high-fidelity solvers, even in a black-box fashion [2]. Specifically, the solid and fluid problems are solved at each time step, and the pressure, velocity and displacements at the interface are communicated in-between to satisfy dynamic, kinematic and geometric coupling conditions respectively. When dealing with situations where the coupling is not very strong, i.e when the effect of one subproblem (e.g solid) on the coupling is significantly less important than the other (e.g fluid), "explicit" schemes, also called "loosely coupled schemes" solve each subproblem only once at each time step, which proved to provide good results in numerous "mildly-coupled" problems (e.g aeroelasticity) [16]. However, in situations that involve strong fluid-structure coupling, these schemes may be unstable [19, 4, 9]. The coupling constraint needs to be enforced more strongly in an implicit way, involving a fixed-point problem solved using an inner loop of subiterations at each time step [6, 7, 2]. This pinpoints the core reason why strongly coupled FSI simulations have a high computational cost.
Reduced Order Models (ROM) enable efficient computations by reducing large systems, and are now more and more used in industrial applications. The proper orthogonal decomposition (POD) is one of the most used ingredients in reduced order modeling. The POD extracts low dimensional linear subspaces from HF data usually obtained with HF simulation results. A ROM can then be built by projecting the FOM equations on the low-order POD basis [21, 15, 3, 22]. Projections methods (e.g POD-Galerkin projection) require knowledge of the governing equations. For that reason, they are considered as Physics-based models. Technically speaking, the projection process requires the access of the source code. The code-intrusive feature of projection-based ROMs can be a shortcoming of their applicability. Recently, some non-intrusive ROMs have been used in FSI problems using different approaches, for example linear interpolation of the POD modes and coefficients for parameterized problems [20], or radial-basis function interpolation of POD coefficients in the context of immersed-shell methods [25]. Hybrid methods combining machine learning algorithms and POD were also used to construct ROMs for FSI [11, 12, 17].
In this work, we focus on cases where one solver (solid) has a significantly greater computational cost than the other (fluid). This is true for example when the structural nonlinear problem is modeled as a quasi-static one (inertial effects neglected). In these conditions, a large-scale nonlinear problem has to be solved several times within a FSI fixed-point iterative loop at each time step. This needs the design of a ROM-FOM coupling approach where a structural ROM predicts the response of the FOM solver in a modular fashion, i.e communicating the displacement and/or the velocity at the interface, from the fluid viscous and pressure forces taken as input.

2 ROM-FOM fluid-structure interaction coupling

A general FSI problem involving an incompressible fluid flow under an ALE description, and an hyperelastic solid can be described by the following systems of equations for each subproblem :

- incompressible Navier-Stokes in the ALE frame:

$$\begin{cases} \rho_f \dfrac{\partial \boldsymbol{v}}{\partial t}_{|\tilde{\mathcal{A}}} + \rho_f \left[(\boldsymbol{v}-\boldsymbol{w}).\nabla\right]\boldsymbol{v} + \nabla p - 2\,\mathbf{div}(\mu_f\,\boldsymbol{D}(\nabla \boldsymbol{v})) = 0 \quad \text{in } \Omega_f(t) \\ \nabla \cdot \boldsymbol{v} = 0 \quad \text{in } \ \Omega_f(t) \\ (2\mu_f\,\boldsymbol{D}(\nabla \boldsymbol{v}) - p\,\boldsymbol{I})\,\boldsymbol{n}_f = \boldsymbol{g}_{N,f} \text{ in } \Gamma_{N,f}(t) \end{cases} \tag{1}$$

  added with wall no slip boundary conditions, imposed velocity profile at inflow boundary conditions and imposed pressure at outflow boundary conditions.

- the equilibrium and constitutive equations for a hyperelastic solid:

$$\begin{cases} \nabla_{\boldsymbol{X}} \boldsymbol{P} = \boldsymbol{0} \quad \text{in } \Omega_s \\ \boldsymbol{P} = \dfrac{\partial W}{\partial \boldsymbol{F}} \\ \boldsymbol{u} = \boldsymbol{0} \quad \text{in } \Gamma_{D,s} \\ \boldsymbol{P}\cdot\boldsymbol{N}_s = \boldsymbol{G}_{N,s} \quad \text{in } \Gamma_{N,s} \end{cases} \tag{2}$$

- the coupling conditions:

$$\begin{cases} \boldsymbol{v} = \dfrac{\partial \boldsymbol{u}}{\partial t} = \boldsymbol{w} \quad \text{on } \Gamma \\ J^{-1}\boldsymbol{F}^T\boldsymbol{P}\cdot\boldsymbol{n}_s + (2\mu_f\,\boldsymbol{D}(\nabla \boldsymbol{v}) - p\,\boldsymbol{I})\cdot\boldsymbol{n}_f = \boldsymbol{0} \quad \text{on } \Gamma_{fsi}(t) \end{cases} \tag{3}$$

with ρ_f the fluid density, μ_f the fluid dynamic viscosity, $\boldsymbol{v}$ is the Eulerian fluid velocity and $\boldsymbol{D}(\nabla \boldsymbol{v})$ is the fluid strain rate tensor. The fluid equations are described on a moving domain (using the ALE moving frame) $\Omega_f(t)$. The Neumann boundary conditions are defined on the moving boundary $\Gamma_{N,f}(t)$ where $\boldsymbol{n}_f$ represents its exterior normal unit vector.
For the solid problem, the equations are written in the Lagrangian frame with $\nabla_{\boldsymbol{X}}\cdot$ the gradient operator in the original configuration, $\boldsymbol{F}$ the deformation gradient and J its determinant. The matrix $\boldsymbol{P}$ is the first Piola-Kirchoff stress tensor and $\Gamma_{D,s}$ and $\Gamma_{N,s}$ are the Dirichlet and Neumann boundaries respectively, in the original configuration as well, whereas $\boldsymbol{n}_s$ is the normal vector in the *current* configuration. The vector field $\boldsymbol{u}$ is the solid displacement field and $\boldsymbol{G}_{N,s}$ is the traction force in the original configuration. The material model is described in the stored energy density function W.
The notation $\tilde{\mathcal{A}}$ represents the ALE mapping from the reference domain (e.g the initial configuration) to the computational domain and $\boldsymbol{w}$ is the ALE velocity, and Γ_{fsi} refers to the "*wet* interface", where coupling between the solid and fluid happens.
As already mentioned above, in this paper we only consider quasi-static solid conditions meaning that the acceleration term is supposed to be negligible, so we get

the elliptic solid problem (2). We consider situations where a quasi-static loading is applied, resulting in steady-state nonlinear problems. In this context, the dynamics of the solid do not affect the global FSI problem, and thus are neglected. The solid displacement, however, still affects the strength of the FSI coupling.

In the context of partitioned FSI simulations, we will use the *Dirichlet-Neumann* coupling formulation that allows a 'black-box' FSI coupling. We represent the fluid solver operation as $\mathcal{F}$:

$$\mathcal{F} : \mathbb{R}^N \rightarrow \mathbb{R}^N \; ; \; \boldsymbol{u}_{|\Gamma_{fsi}} \rightarrow \boldsymbol{f}_{|\Gamma_{fsi}} \tag{4}$$

where $\boldsymbol{u}_{|\Gamma_{fsi}}$ is the displacement field and $\boldsymbol{f}_{|\Gamma_{fsi}}$ represents the fluid viscous and pressure forces at Γ_{fsi}:

$$\boldsymbol{f}_{|\Gamma_{fsi}} = (2\mu_f \boldsymbol{D}(\nabla \boldsymbol{v}) - p\boldsymbol{I}) \cdot \boldsymbol{n}_{f|\Gamma_{fsi}}. \tag{5}$$

Similarly, the solid operator is defined as:

$$\mathcal{S} : \mathbb{R}^N \rightarrow \mathbb{R}^N \; ; \; \boldsymbol{f}_{|\Gamma_{fsi}} \rightarrow \boldsymbol{u}_{|\Gamma_{fsi}}. \tag{6}$$

In fully implicit schemes, the coupling conditions can be enforced using a fixed-point formulation of the problem (1)-(3):

$$(\mathcal{F} \circ \mathcal{S})(\boldsymbol{f}_{|\Gamma_{fsi}}) = \boldsymbol{f}_{|\Gamma_{fsi}}. \tag{7}$$

One approach to solve (7) at each time step is to compute Picard iterations plus a fixed-point acceleration using Quasi-Newton methods for the FSI problem:

$$(\mathcal{F} \circ \mathcal{S})(\boldsymbol{f}_{|\Gamma_{fsi}}) - \boldsymbol{f}_{|\Gamma_{fsi}} = \boldsymbol{0} \tag{8}$$

(We use here the interface-quasi-Newton with inverse Jacobian from a least-squares model (IQN-ILS) as the acceleration method [6], along with the filtering method used in [13]). We use the software library `preCICE` [5] as a coupling interface for the simulations.

2.1 Non-intrusive model order reduction strategy

The goal of the ROMs used in this work is to reduce the overall computational cost of the FSI problem through the order reduction of the solid subproblem only. Using partitioned FSI schemes allows for the replacement of the "*module*" of the solid solver $\mathcal{S}$ with a new ROM solver $\mathcal{S}'$:

$$\mathcal{S}' : \mathbb{R}^N \rightarrow \mathbb{R}^N \; ; \; \boldsymbol{f}_{|\Gamma_{fsi}} \rightarrow \hat{\boldsymbol{u}}_{|\Gamma_{fsi}} \tag{9}$$

and thus achieving a non-intrusive implementation of the model reduction. In fact, the suggested ROM will also be able to predict the full displacement field (and stress and strain tensor fields) in addition to the interface displacement. But note that only the interaction variables located at the FSI interface are needed to advance the FSI solution in time. The fluid solver, as well as the other components of the FSI algorithm (i.e implicit coupling, Quasi-Newton acceleration ...) remain the same. This produces a non-intrusive ROM-FOM coupling scheme, with a reduced computational cost than the original FOM-FOM coupling.

It's worth mentioning that this strategy can particularly achieve significant speedups when the solid FOM is much more expensive than the fluid FOM. Moreover, we assume that in online-computations, the average number of subiterations does not increase compared to the FOM-FOM problem. As we will see in the numerical experiments, this is the case when the solid ROM is accurate enough and stable compared to the FOM.

2.1.1 Expected speedups

In this short section, we give an idea of the overall speedup (denoted by s) of the partitioned FSI coupling if the solid ROM solver returns a speedup σ compared to the solid FOM solver. As mentioned above we will assume that the number of fixed-point subiterations does not vary between FOM-FOM and FOM-ROM strategies. Let us denote by T_f (resp. T_s) the mean computational time taken by the FOM fluid (resp. solid) solver during one time iteration of the FSI coupling. The total FOM-FOM time over a time step is $T_f + T_s$ while the FOM-ROM time is $T_f + T_s/\sigma$. The FOM-ROM speedup is then

$$s = \frac{T_f + T_s}{T_f + \dfrac{T_s}{\sigma}} = \frac{1 + T_s/T_f}{1 + \dfrac{1}{\sigma} T_s/T_f}.$$

Assume that $T_s/T_f \gg 1$. Then we get the speedup estimation

$$s \approx \frac{T_s/T_f}{1 + \dfrac{1}{\sigma} T_s/T_f} = \frac{\sigma}{1 + \sigma \dfrac{T_f}{T_s}}. \tag{10}$$

Equation (10) shows that a 'good' solid ROM speedup should be of the order T_s/T_f. Assume for example that $\sigma = T_s/T_f$, then one finds $s = \sigma/2$ and the efficiency of the FOM-ROM FSI strategy is $1/2$. More generally, if the solid ROM achieves a solid speedup $\sigma = \alpha \dfrac{T_s}{T_f}$ with $\alpha > 0$, then $s \approx \left(1 - \dfrac{1}{1+\alpha}\right) \dfrac{T_s}{T_f}$. In particular, the ratio $\dfrac{T_s}{T_f}$ is an upper bound of FOM-ROM FSI speedup.

2.1.2 FOM-ROM algorithm

Since we are interested in solid problems with quasi-static behaviour only, we argue that the solid ROM can ignore the dynamics effects and only take into account the fluid loading at the interface.
The HF solution from the FOM-FOM coupling is first used to train our model. Accordingly, two snapshot matrices are created from the forces the interface $\boldsymbol{F}$ and the full solid displacement field $\boldsymbol{U}$, collecting snapshot solutions from *all* the subiterations at each time step during the FOM computation. We note that the force field is discretised on the solid mesh interface, meaning that we collect the force data after the mesh mapping step during the FSI solution schemes.
The suggested ROM performs a dimensionality reduction of the input $\boldsymbol{f}_{|\Gamma_{fsi}}$ and output $\hat{\boldsymbol{u}}$ of the solver, and then solves a regression problem in the low-order latent space. Specifically, we use the Principal Component Analysis (PCA) method to find

the best subspace of rank r on which those fields are projected, we will refer to these PCA modes as $\boldsymbol{\Phi}_f \in \mathbb{R}^{N \times r_f}$ and $\boldsymbol{\Phi}_u \in \mathbb{R}^{N_s \times r_u}$ respectively, where N_s is the number of displacement degrees of freedom in the solid domain. The regression problem on the other hand can be solved using different existing methods:

$$\mathcal{I} : \mathbb{R}^{r_f} \rightarrow \mathbb{R}^{r_u} \; ; \; \tilde{\boldsymbol{f}} \rightarrow \tilde{\boldsymbol{u}} \tag{11}$$

where $\tilde{\boldsymbol{f}} = \boldsymbol{\Phi}_f^T \boldsymbol{f}_{|\Gamma_{fsi}}$ and $\tilde{\boldsymbol{u}} = \boldsymbol{\Phi}_u^T \boldsymbol{u}$ are the coordinates of the force field and the displacement field in the reduced bases respectively. In our experiments, the regression methods that provided the best accuracy are reduced basis function (RBF) interpolation [23] and low-degree polynomial approximation (degree less than three).

In the offline step, $\boldsymbol{\Phi}_f \in \mathbb{R}^{N \times r_f}$ and $\boldsymbol{\Phi}_u \in \mathbb{R}^{N_s \times r_u}$ are computed using the SVD of $\boldsymbol{F}$ and $\boldsymbol{U}$ respectively, the numbers of modes kept r_f and r_u can be chosen using a variance energy threshold (e.g keeping 99.99% of the energy). The coordinates of the data points in the discrete reduced bases $\tilde{\boldsymbol{F}} = \boldsymbol{\Phi}_f^T \boldsymbol{F}$ and $\tilde{\boldsymbol{U}} = \boldsymbol{\Phi}_u^T \boldsymbol{U}$ respectively will be used to learn the surrogate model $\mathcal{I}(\tilde{\boldsymbol{F}}) = \tilde{\boldsymbol{U}}$. Note that the numbers of modes used will directly affect the quality of this regression model. In fact, keeping too much modes might result in a too big of a dimensionality for the surrogate $\mathcal{I}(\cdot)$ to have a good predictive ability with the available data. Keeping too few modes induces a loss of information both at the "encoding" and the "decoding" part of the ROM. On the online phase, at each subiteration, the solid ROM receives a new interface force $\boldsymbol{f}_{|\Gamma_{fsi},current}$, its projection on the reduced basis is computed $\tilde{\boldsymbol{f}}_{current} = \boldsymbol{\Phi}_f^T \boldsymbol{f}_{|\Gamma_{fsi},current}$. The regression model then rapidly predicts the coordinates of the current displacement field on the reduced basis $\tilde{\boldsymbol{u}}_{current} = \mathcal{I}(\tilde{\boldsymbol{f}}_{current})$. A reverse projection on the high-dimensional space then gives the full displacement field $\hat{\boldsymbol{u}}_{current} = \boldsymbol{\Phi}_u \tilde{\boldsymbol{u}}_{current}$.

2.2 Example 1: one-dimensional elastic arterial vessel model

The model of flexible tube and related HF partitioned solvers proposed by [7] are used here. The fluid is assumed be incompressible with constant density ρ. Both fluid mass and momentum conservation equations read

$$\begin{cases} \partial_t a + \partial_x (av) = 0, \\ \partial_t (av) + \partial_x (av^2) + \dfrac{a}{\rho} \partial_x p = 0, \quad t > 0, \; x \in [0, L] \end{cases} \tag{12}$$

where v is the bulk velocity, a is the tube cross section and p is the pressure. From the fluid side, the unknowns are both velocity and pressure. For the solid flexible tube, an algebraic quasi-static model

$$a = a(p)$$

is used (retaining only the tube stress in the circumferential direction). The following nonlinear elastic stress-strain law is used:

$$\begin{cases} \sigma_{\varphi\varphi} = 12500\, \epsilon_{\varphi\varphi} \quad \text{if } |\epsilon_{\varphi\varphi}| < \epsilon_0 \\ \sigma_{\varphi\varphi} = 2500\, \epsilon_{\varphi\varphi} + 20 \quad \text{if } \epsilon_{\varphi\varphi} \geq \epsilon_0 \\ \sigma_{\varphi\varphi} = 2500\, \epsilon_{\varphi\varphi} - 20 \quad \text{if } \epsilon_{\varphi\varphi} \leq -\epsilon_0 \end{cases} \tag{13}$$

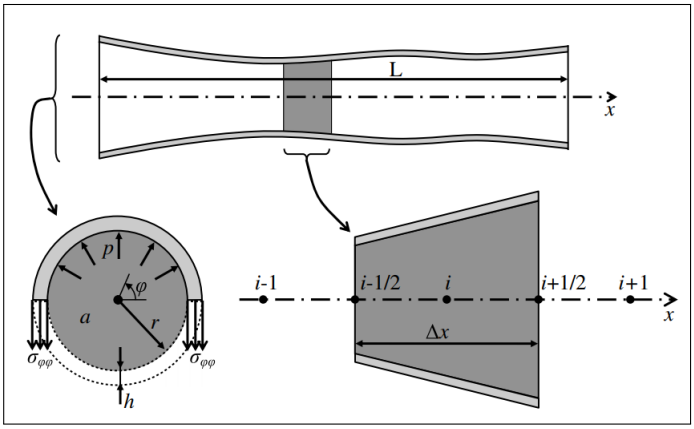

Figure 1: Arterial vessel test case schematic explanation (from [7])

with $\epsilon_0 = 2\ 10^{-3}$ for the numerical experiments. Figure 2.2 shows a schematic explanation of this problem. A non-reflective boundary condition is used on the right boundary as suggested in [7]. The prescribed inlet (left face) velocity is computed using the solution of a nonlinear Duffing equation in order to produce a signal with rather complex dynamics:

$$\begin{cases} \ddot{u}(t) = a\,u(t) + b\,u^2(t) + c\,u^3(t) + d + p\,\cos(ft) + e\,\dot{u}(t) \quad \forall t \in [0,T] \\ u(0) = 10 \ ; \ \dot{u}(0) = 0, \\ v_{inlet}(t) = gu(t) + h. \end{cases} \tag{14}$$

We use $T = 120$ s and fix the coefficients

$$(a,\ b,\ c,\ d,\ e,\ g,\ p) = (-1,\ 0,\ -0.002,\ -1,\ -0.02,\ 1/60,\ 360).$$

We consider the parameter vector $\boldsymbol{\mu} = (f\ \ , h)^T$ for the generation of different frequencies and amplitudes. In order to train the ROM model, a FOM-FOM computation is done on a single inlet velocity case corresponding to $\boldsymbol{\mu}_1 = (2\ \ , 6)^T$ (see Figure 2.2), for a simulation time period $t \in [0, 18]$ s. The fluid flow equations (12) are solved using a second order finite volume scheme with a constant time step $\Delta t = 0.1$ s, and the solid section $a(p)$ is computed at each iteration as the solution of a scalar minimization problem. Four modes are selected for both force and displacement modes, and a thin plate spline kernel RBF interpolator is used [24]. After the ROM has been trained, we test the ROM-FOM coupling on the future prediction of the problem at the same inlet velocity, and then we test it on a different prescribed velocity corresponding to $\boldsymbol{\mu}_2 = (0.9\ \ , 4)^T$. We can see the difference between the two signals in Figure 2.2.. The results for theses two cases are shown in Figures 2.2. and 2.2. respectively, compared to the HF FOM-FOM solution. We can see a significant accuracy achieved by the suggested ROM. Moreover, we show the stress-strain law reconstructed using the ROM-FOM simulation in Figure 2.2., showing that the proposed ROM approach can capture the solid problem nonlinearities. Remarkably, we can also see that the ROM-FOM successfully predicted the tube response in an extrapolated region in the strain response (strain region $\epsilon_{\varphi\varphi} < -0.0055$) even for this nonlinear constitutive law, although it should

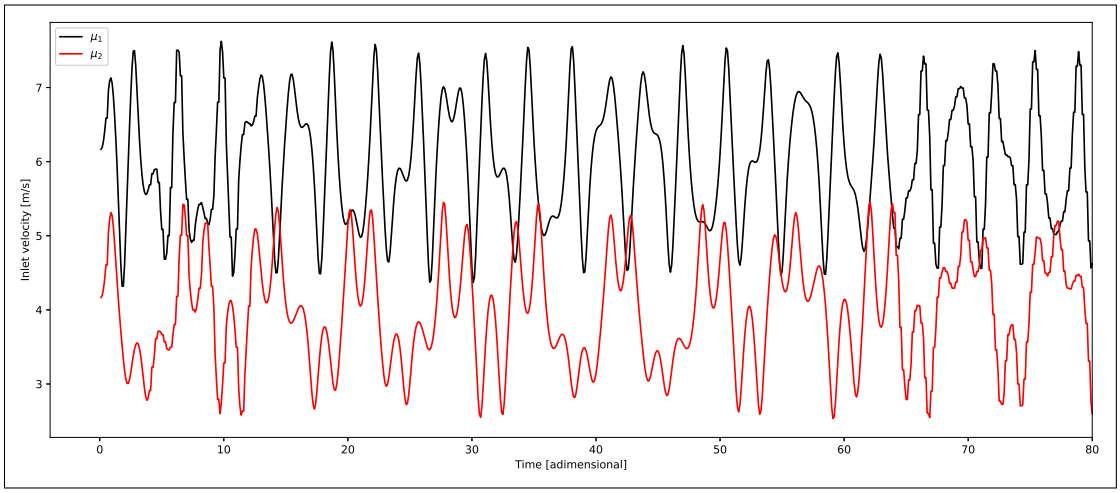

Figure 2: Inlet velocity signals corresponding to $\boldsymbol{\mu}_1$ and $\boldsymbol{\mu}_2$. For the training phase we use $\boldsymbol{\mu}_1$ in the $t \in [0, 18s]$ time window. For the prediction, we use $\boldsymbol{\mu}_2$ and $\boldsymbol{\mu}_1$ for $t \geq 18s$.

be noted that it only involves a linear extrapolation from the phase space seen in the training.

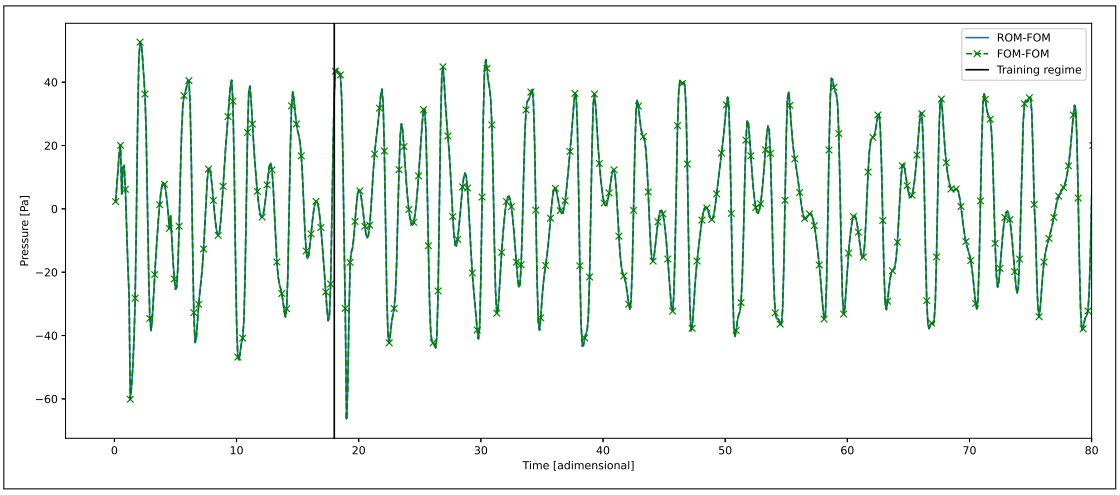

Figure 3: The inlet pressure solution using the FOM-FOM (green dashed line with cross marks) and the ROM-FOM (blue solid line). Prescribed inlet velocity corresponding to $\boldsymbol{\mu}_1$. Training and prediction regimes. The vertical black line indicates the end of the training time period.

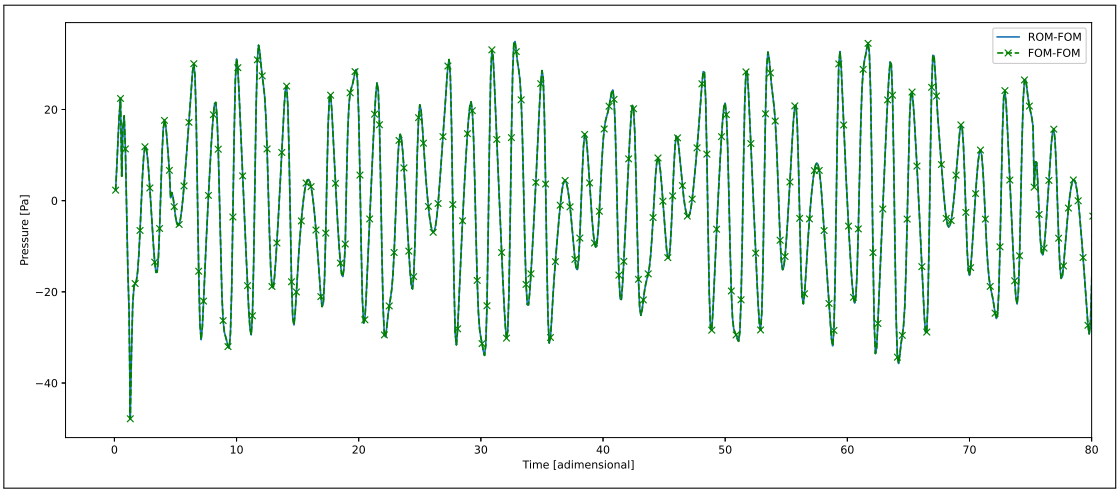

Figure 4: The inlet pressure solution using the FOM-FOM and the ROM-FOM. Prescribed inlet velocity corresponds to $\boldsymbol{\mu}_2$. Prediction regime.

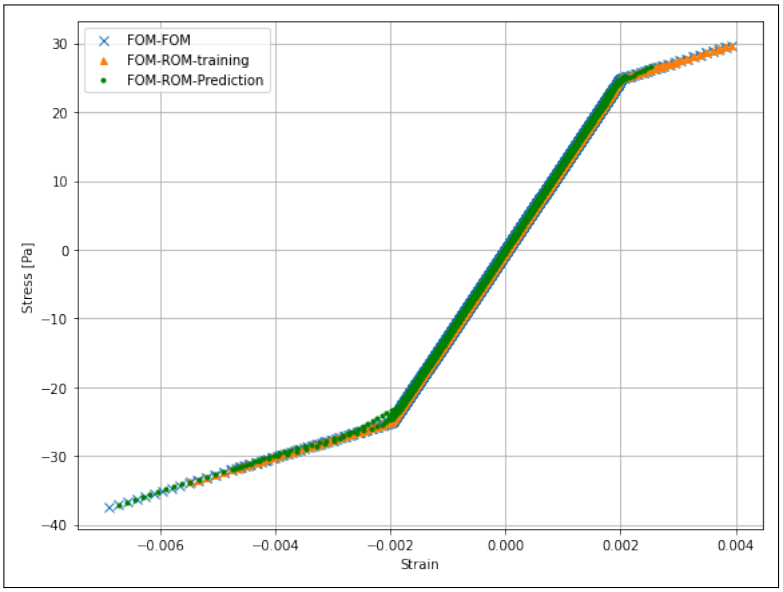

Figure 5: Nonlinear elastic Stress-Strain law used for the vessel tube. The reconstructed curve from the ROM-FOM prediction is plotted along with the FOM-FOM model. We can also see the data points from the FOM-FOM simulation used for the ROM training.

3 Concluding remarks and perspectives

We have presented a ROM-FOM coupling strategy to reduce the computational cost of partitioned FSI simulations, through the reduction of the solid quasi-static sub-problem when the cost of the solid solver is predominant. The proposed approach can be implemented in a totally non-intrusive way. Using POD for the dimensionality

reduction of the fluid forces as well as the displacement field, then a regression model between the two fields in the latent space, the solid ROM has been shown to accurately predict the full displacement field online with a significant speedup. We have demonstrated the ability of the proposed ROM strategy on the problem of the FSI arterial vessel, where we show a significant accuracy even for complex dynamics, these properties are also seen in an extrapolated region in both time and parametric spaces.

In future works, we envision to apply this ROM-FOM strategy on more computationally heavy test cases for 2D and 3D problems. We have promising early results on a 2D FSI coupling case between a quasi-static hyperelastic plane strain solid and an incompressible flow facing a cylinder. A Reynolds number of $Re = 250$ was used for training, although the testing can be done on different -though close- Reynolds numbers, i.e Re plays the role of $\boldsymbol{\mu}$ in the previous test case. As seen in Figure 6, the presence of the cylinder induces a vortex street, making the fluid dynamics more complex (chaotic), even in the absence of solid dynamical effects. We note that our strategy can be extended quite naturally and with minimal to no modifications for two-dimensional problems. In this case for example, the same quasi-Newton fixed point algorithm is used, and a polynomial regression of the 2^{nd} order was used as interpolation. More fluid basis functions are typically needed for these problems to capture the nonlinearities of the interfacial forces. Here, the solid FOM is 1.7 more computationally expensive than the fluid FOM ($\frac{T_s}{T_f} = 1.7$), and the ROM strategy returns a solid ROM speedup of $\sigma \approx 760$, making the overall speedup $s \approx 1.69$. We expect a stronger speedup in the 3D case because of the computational cost of nonlinear quasi-static structural models.

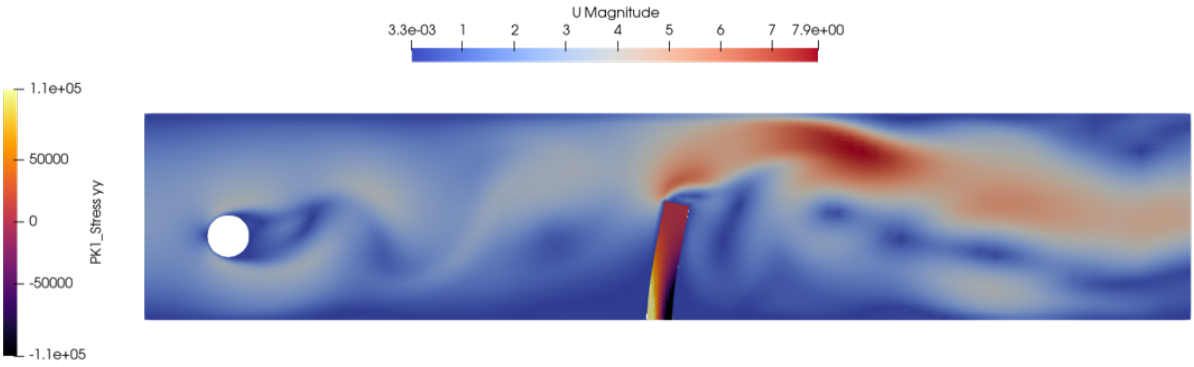

Figure 6: A snapshot of the FOM-ROM solution for the test case of FSI between a hyperelastic solid and an incompressible viscous flow. A rigid obstacle is included to generate van Karman alleys and make the flow regime chaotic.

Acknowledgements

This work has been funded by the ANR (Agence Nationale de la Recherche), Altair Engineering and Michelin.

References

[1] Klaus-Jürgen Bathe and Hou Zhang. Finite element developments for general fluid flows with structural interactions: GENERAL FLUID FLOWS WITH STRUCTURAL INTERACTIONS. *International Journal for Numerical Methods in Engineering*, 60(1):213–232, 2004.

[2] A. E. J. Bogaers, S. Kok, B. D. Reddy, and T. Franz. Quasi-Newton methods for implicit black-box FSI coupling. *Computer Methods in Applied Mechanics and Engineering*, 279:113–132, September 2014.

[3] T. Bui-Thanh, K. Willcox, and O. Ghattas. Parametric Reduced-Order Models for Probabilistic Analysis of Unsteady Aerodynamic Applications. *AIAA Journal*, 46(10):2520–2529, October 2008. Publisher: American Institute of Aeronautics and Astronautics.

[4] P. Causin, J. F. Gerbeau, and F. Nobile. Added-mass effect in the design of partitioned algorithms for fluid–structure problems. *Computer Methods in Applied Mechanics and Engineering*, 194(42):4506–4527, October 2005.

[5] Gerasimos Chourdakis, Kyle Davis, Benjamin Rodenberg, et al. precice v2: A sustainable and user-friendly coupling library. *Open Research Europe*, 2(51), September 2022.

[6] Joris Degroote, Klaus-Jürgen Bathe, and Jan Vierendeels. Performance of a new partitioned procedure versus a monolithic procedure in fluid–structure interaction. *Computers & Structures*, 87(11-12):793–801, June 2009.

[7] Joris Degroote, Peter Bruggeman, Robby Haelterman, and Jan Vierendeels. Stability of a coupling technique for partitioned solvers in FSI applications. *Computers & Structures*, 86(23-24):2224–2234, December 2008.

[8] J. Donea, S. Giuliani, and J. P. Halleux. An arbitrary lagrangian-eulerian finite element method for transient dynamic fluid-structure interactions. *Computer Methods in Applied Mechanics and Engineering*, 33(1):689–723, September 1982.

[9] Carlos A. Felippa, K. C. Park, and Charbel Farhat. Partitioned analysis of coupled mechanical systems. *Computer Methods in Applied Mechanics and Engineering*, 190(24):3247–3270, March 2001.

[10] Miguel A. Fernández and Jean-Frédéric Gerbeau. Algorithms for fluid-structure interaction problems. In Luca Formaggia, Alfio Quarteroni, and Alessandro Veneziani, editors, *Cardiovascular Mathematics: Modeling and simulation of the circulatory system*, MS&A, pages 307–346. Springer Milan, Milano, 2009.

[11] Stefania Fresca and Andrea Manzoni. POD-DL-ROM: Enhancing deep learning-based reduced order models for nonlinear parametrized PDEs by proper orthogonal decomposition. *Computer Methods in Applied Mechanics and Engineering*, 388:114181, January 2022.

[12] Rachit Gupta and Rajeev Jaiman. A hybrid partitioned deep learning methodology for moving interface and fluid–structure interaction. *Computers & Fluids*, 233:105239, January 2022.

[13] R. Haelterman, A. E. J. Bogaers, K. Scheufele, B. Uekermann, and M. Mehl. Improving the performance of the partitioned QN-ILS procedure for fluid–structure interaction problems: Filtering. *Computers & Structures*, 171:9–17, July 2016.

[14] Matthias Heil. An efficient solver for the fully coupled solution of large-displacement fluid–structure interaction problems. *Computer Methods in Applied Mechanics and Engineering*, 193(1):1–23, January 2004.

[15] Toni Lassila, Andrea Manzoni, Alfio Quarteroni, and Gianluigi Rozza. Model Order Reduction in Fluid Dynamics: Challenges and Perspectives. In Alfio Quarteroni and Gianluigi Rozza, editors, *Reduced Order Methods for Modeling and Computational Reduction*, MS&A - Modeling, Simulation and Applications, pages 235–273. Springer International Publishing, Cham, 2014.

[16] Michel Lesoinne and Charbel Farhat. Geometric conservation laws for flow problems with moving boundaries and deformable meshes, and their impact on aeroelastic computations. *Computer Methods in Applied Mechanics and Engineering*, 134(1):71–90, July 1996.

[17] T. P. Miyanawala and Rajeev K. Jaiman. A Hybrid Data-Driven Deep Learning Technique for Fluid-Structure Interaction. In *ASME 2019 38th International Conference on Ocean, Offshore and Arctic Engineering*. American Society of Mechanical Engineers Digital Collection, November 2019.

[18] Scott A. Morton, Reid B. Melville, and Miguel R. Visbal. Accuracy and Coupling Issues of Aeroelastic Navier-Stokes Solutions on Deforming Meshes. *Journal of Aircraft*, 35(5):798–805, September 1998. Publisher: American Institute of Aeronautics and Astronautics.

[19] Fabio Nobile. *Numerical approximation of fluid-structure interaction problems with application to haemodynamics*. PhD thesis, EPFL, Lausanne, 2001.

[20] Vilas Shinde, Elisabeth Longatte, Franck Baj, Yannick Hoarau, and Marianna Braza. Galerkin-free model reduction for fluid-structure interaction using proper orthogonal decomposition. *Journal of Computational Physics*, 396:579–595, November 2019.

[21] Lawrence Sirovich. Turbulence and the dynamics of coherent structures. II. Symmetries and transformations. *Quarterly of Applied Mathematics*, 45(3):573–582, 1987.

[22] Karen Veroy, Christophe Prud'homme, Dimitrios Rovas, and Anthony Patera. A Posteriori Error Bounds for Reduced-Basis Approximation of Parametrized Noncoercive and Nonlinear Elliptic Partial Differential Equations. In *16th AIAA Computational Fluid Dynamics Conference*. American Institute of Aeronautics and Astronautics, 2012.

[23] Grace Wahba. *Spline Models for Observational Data*. CBMS-NSF Regional Conference Series in Applied Mathematics. Society for Industrial and Applied Mathematics, January 1990.

[24] Simon N. Wood. Thin Plate Regression Splines. *Journal of the Royal Statistical Society Series B: Statistical Methodology*, 65(1):95–114, August 2003.

[25] D. Xiao, P. Yang, F. Fang, J. Xiang, C. C. Pain, and I. M. Navon. Non-intrusive reduced order modelling of fluid–structure interactions. *Computer Methods in Applied Mechanics and Engineering*, 303:35–54, May 2016.